

# A FRAMEWORK FOR DYNAMIC APERTURE STUDIES FOR COLLIDING BEAMS IN THE HIGH-LUMINOSITY LARGE HADRON COLLIDER\*

S. Kostoglou<sup>†</sup>, H. Bartosik, R. De Maria, Y. Papaphilippou, G. Sterbini, CERN, Geneva, Switzerland

## Abstract

During the last physics run of the Large Hadron Collider (LHC), Dynamic Aperture (DA) studies have been successfully employed to optimize the accelerator's performance by guiding the selection of the beam and machine parameters. In this paper, we present a framework for single-particle tracking simulations aiming to refine the envisaged operational scenario of the future LHC upgrade, the High-Luminosity LHC (HL-LHC), including strong non-linear fields such as beam-beam interactions. The impact of several parameters and beam processes during the cycle is initially illustrated with frequency maps and then quantified with DA studies.

## INTRODUCTION

The High-Luminosity Large Hadron Collider (HL-LHC) aims to reach an integrated luminosity of  $250 \text{ fb}^{-1}$  per year in the two high-luminosity experiments ATLAS and CMS [1]. Achieving such a goal is feasible as a result of the increased beam intensity provided by the injectors, the Achromatic Telescopic Squeeze (ATS) optics that allow for a smaller beam size at the Interaction Points (IPs) 1 and 5 and the development of novel technologies for beam manipulation, such as the  $\text{Nb}_3\text{Sn}$  magnets for the final beam focusing and the crab cavities [1–3].

Apart from these innovative techniques, the performance of the accelerator strongly depends on the orchestration of several beam and machine parameters during the cycle. To study the crucial impact of such parameters on the single-particle beam dynamics, a framework for multi-parametric Dynamic Aperture (DA) scans has been developed and successfully employed since Run 2 [4, 5]. Based on single-particle tracking simulations, these tools guide the selection of the appropriate configuration for operation, optimize the performance of the accelerator and validate the envisaged operational scenario for future runs.

The goal of the present paper is to determine the feasibility of the proposed operational baseline for the first operation run in the HL-LHC era (Run 4) [6] through DA simulations and provide an understanding of the underlying mechanisms that lead to a degradation of the DA and thus, of the beam lifetime. Our primary focus lies on the beam collisions, being the most critical beam process in the cycle due to the presence of strong non-linear fields produced by beam-beam interactions.

\* Research supported by the HL-LHC project.

<sup>†</sup> sofia.kostoglou@cern.ch

## SIMULATION FRAMEWORK

The single-particle symplectic tracking code, SixTrack, is employed for the tracking simulations [7]. A single beam is tracked element-by-element in the HL-LHC lattice that corresponds to Beam 1. Important non-linearities induced by the chromaticity sextupoles, the Landau octupoles and both the head-on and long-range beam-beam encounters are considered. The weak-strong approximation is used to treat beam-beam effects as the charge distribution of the opposite beam (Beam 2) is considered unperturbed.

For the DA studies, an initial distribution forming a polar grid that extends up to  $10 \sigma$  with 5 angles in the configuration space  $(x, y)$  is tracked for a maximum of  $10^6$  turns, which corresponds to a duration of approximately 90 seconds of the accelerator's operation. Longitudinally, the particles are placed at a momentum offset corresponding to  $3/4$  of the RF bucket height and the simulations include the effect of the synchrotron motion. The main observable is the minimum DA across the angles that form the initial distribution. The number of angles is increased to 49 for the computation of the frequency maps. A selection of parameters used in the simulations is summarized in Table 1.

Table 1: HL-LHC Baseline Simulation Parameters During Collisions [6]

Parameters (Unit)	HL-LHC (Values)
Beam energy (TeV)	7
RMS bunch length (cm)	9
Coupling $ C^- $	$10^{-3}$
Normalised emittance (m rad)	2.5
Chromaticity $Q'_{x,y}$	15
IP1/5 half crossing angle (rad)	250
IP2/8 half crossing angle (rad)	170
IP8/2 $\beta_{x,y}^*$ (m)	1.5/10
Relative momentum deviation $\delta p/p$	$27 \times 10^{-5}$
Start of luminosity leveling	
Bunch population (protons)	$2.3 \times 10^{11}$
Landau octupoles' current (A)	410
IP1/5 $\beta_{x,y}^*$ (m)	1
End of luminosity leveling	
Bunch population (protons)	$1.3 \times 10^{11}$
Landau octupoles' current (A)	100
IP1/5 $\beta_{x,y}^*$ (m)	0.2
ATS-factor	2.5
Half crab-cavity angle (rad)	190

## START OF $\beta^*$ -LEVELING

To maintain a constant luminosity of  $5 \times 10^{34} \text{ cm}^{-2}\text{s}^{-1}$  during proton collisions, luminosity leveling techniques are employed, i.e.,  $\beta^*$  in IP1 and IP5 are gradually reduced to compensate for the proton intensity decay resulting from the collision process. The luminosity leveling begins with  $\beta^* = 1 \text{ m}$ , the maximum bunch intensity and positive octupole current as presented in Table 1.

Figure 1 illustrates the Frequency Map Analysis (FMA) [8–12] for the start of the luminosity leveling. For the frequency maps, a distribution of particles is tracked for  $10^4$  revolutions and the turn-by-turn data of the first and last 2000 turns are used to compute the tune of each particle. The comparison of the tunes at these two-time intervals defines the tune diffusion and a color code is assigned to its value. The considered working point (without beam-beam effects) is close to the diagonal and equal to  $(Q_x, Q_y) = (62.313, 60.318)$ . The main resonance lines are also shown (gray). An important tune spread due to the head-on beam-beam interactions is observed in combination with a linear detuning from the octupoles.

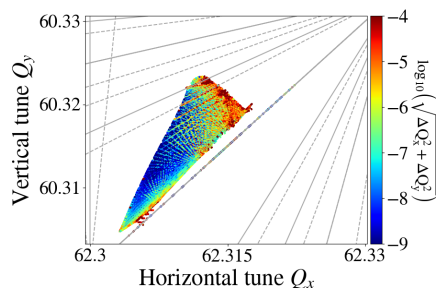


Figure 1: Frequency Map Analysis for the start of  $\beta^*$ -leveling with  $(Q_x, Q_y) = (62.313, 60.318)$ . The color-code indicates the logarithm of the tune diffusion and the main resonance lines are also depicted (gray).

Previous studies have established a correlation between beam lifetime from experimental data and DA from simulations [13]. Based on the experience gained during Run 2 (2015-2018), an operational scenario is characterized as feasible when the two following criteria are satisfied in the simulations: a minimum DA of at least  $6 \sigma$  is achieved along with a tune split, namely the difference between the decimal part of the horizontal and vertical tune, of at least  $5 \times 10^{-3}$  to prevent beam instabilities. Tunes above the diagonal are generally preferred ( $Q_x < Q_y$ ) as there is no experience of operating with working points below the diagonal. Operating below the diagonal may also be prevented due to the additional tune-shift induced by electron-cloud.

To this end, a scan in the tune domain is performed to investigate the existence of working points that fulfill the DA constraints. Figure 2 depicts the horizontal tune as a function of the vertical tune. Each point represents a separate DA simulation and a color code indicates the minimum DA. The diagonal ( $Q_x = Q_y$ ) and the tune split of  $|Q_x - Q_y| > 5 \times 10^{-3}$

are also shown (white and blue lines, respectively). The feasibility criteria are satisfied for a single working point  $(Q_x, Q_y) = (62.316, 60.321)$ .

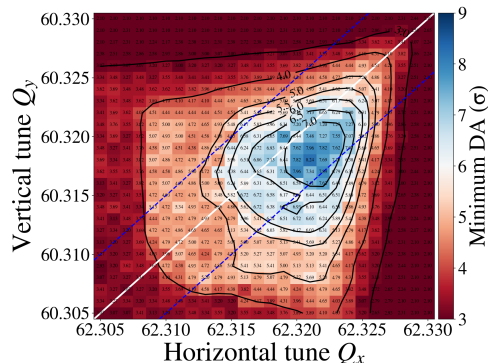


Figure 2: Horizontal tune as a function of vertical tune at the start of  $\beta^*$ -leveling, color-coded with the minimum DA. The diagonal (white line) and the distance of  $5 \times 10^{-3}$  from the diagonal (blue lines) are also illustrated.

## END OF $\beta^*$ -LEVELING

At the end of the luminosity leveling (6.4 h after the start of collisions),  $\beta^*$  is squeezed to 20 cm in the high luminosity experiments (IP1 and IP5). This reduction is achieved with an ATS optics, which is characterized by the ATS factor indicating the ratio between  $\beta^*$  of the pre-squeezed optics and  $\beta^*$ . The ATS factor is equal to 2.5 at the end of the luminosity leveling. The bunch intensity, the settings of the Landau octupoles and the half crab cavity angle in IP1 and IP5 at this stage of the collision process are reported in Table 1.

Figure 3 shows the frequency map at the end of the luminosity leveling. The shape of the footprint indicates that, at this stage of collisions, the dominating factor is the long-range beam-beam effect, while a smaller head-on tune spread is observed due to the decrease of the beam intensity. The DA tune scan at the end of the luminosity leveling is illustrated in Fig. 4. The DA criteria are fulfilled for several working points above the diagonal. A comparison between Figs. 2 and 4 also depicts that, to maintain a minimum DA of at least  $6 \sigma$  across the whole collision process, the working point must be changed during the leveling.

## THE CORRECTION SEXTUPOLES IN Q10

The LHC lattice consists of an uneven number of strong sextupoles adjacent to IP1 and IP5, responsible for the correction of the chromatic aberrations induced by the triplet when squeezing the  $\beta^*$ . The reduction of the transverse beam size in the IP is accompanied by an increase of the  $\beta$ -functions at the sextupole locations, especially in the presence of a large ATS factor, resulting in the excitation of sextupolar resonant driving terms that may impact the DA. Hence, in the HL-LHC baseline the installation of an additional strong sextupole is envisaged, namely the MS10 in the quadrupole

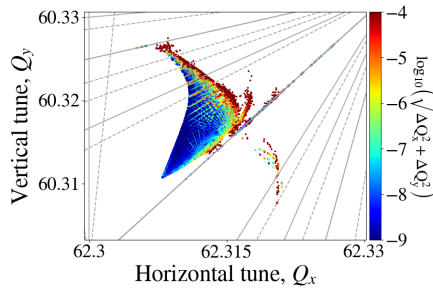


Figure 3: Frequency Map Analysis for the end of  $\beta^*$ -leveling and  $(Q_x, Q_y) = (62.313, 60.318)$ .

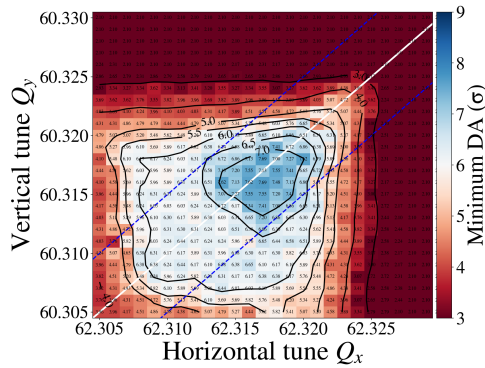


Figure 4: DA tune scan at the end of  $\beta^*$ -leveling.

Q10 of the dispersion suppressor. This would enable, using the even number of sextupoles as pairs with a phase advance of  $\pi$ , to self-compensate for these aberrations. However, due to the complexity of its installation, the following section reviews the DA machine performance at the end of the luminosity leveling assuming no MS10 installation. At the start of collisions, in fact, no significant DA degradation is reported in the absence of MS10 [14].

Figure 5 presents the DA tune scan with an HL-LHC lattice that does not include the MS10. A comparison with Fig. 4 yields a slight shrinkage of the 6 DA island and an overall DA decrease of 0.5. This demonstrates that the installation of MS10 is clearly beneficial for DA. Nevertheless, the DA target is easily reached for several working points above the diagonal even in the absence of MS10. It must be noted that the simulations include the arc orbit bumps (dispersion bumps) responsible for the correction of the dispersion induced by the crossing scheme at the high luminosity IPs, otherwise strong chromatic effects are observed when considering the lattice without MS10 [14].

Previous studies have proposed an optimization of the phase advance between IP1 and IP5 to improve the collider's performance in the absence of MS10 [15]. In particular, simulations without beam-beam effects have shown that a change of 0.05 radians/(2) in both horizontal and vertical phase advance, from (31.38, 30.331) to (31.43, 30.381), is expected to be beneficial for DA. Figure 6 illustrates the DA tune scan in the absence of MS10 with the proposed

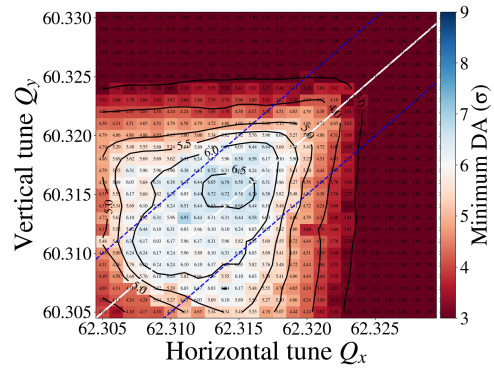


Figure 5: DA tune scan at the end of  $\beta^*$ -leveling in the absence of MS10.

phase advance optimization, including beam-beam effects. A comparison between Figs. 4, 5 and 6 confirms that the DA degradation due to the absence of MS10 can be partially restored by fine-tuning the phase advance between the two IPs.

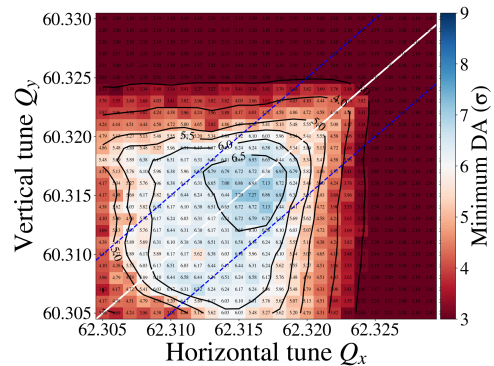


Figure 6: DA tune scan at the end of  $\beta^*$ -leveling in the absence of MS10 with an optimized IP1-5 phase advance.

## CONCLUSIONS

DA simulations including beam-beam effects have been used to study the feasibility of the Run 4 envisaged operational scenario for proton-proton collisions. The results for the two most critical stages of the collision process, the start and the end of the  $\beta^*$ -leveling, indicate that it is possible to reach the DA target with the proposed configuration. Although the existence of the strong sextupole MS10 in Q10 in the arcs adjacent to IP1 and IP5 allows for a more efficient compensation of chromatic aberrations and its installation would be beneficial mainly at the end of the luminosity leveling, the DA is still at acceptable levels even in the absence of MS10 when the dispersion correction bumps are present. In this case, it was demonstrated, as proposed by previous studies, that the impact of not installing MS10 can be partially restored by optimizing the phase advance between IP1-5.

## REFERENCES

- [1] G. Apollinari *et al.*, “High-Luminosity Large Hadron Collider (HL-LHC)”, CERN, Geneva, Switzerland, Rep. CERN-2017-007-M, 2017.
- [2] G. Arduini *et al.*, “Beam parameters at LHC injection”, CERN, Geneva, Switzerland, Rep. CERN-ACC-2014-0006, Jan. 2014.
- [3] S. Fartoukh, “Achromatic telescopic squeezing scheme and application to the LHC and its luminosity upgrade”, *Physical Review Special Topics - Accelerators and Beams*, vol. 16, no. 11, p. 111002, 2013.  
doi:10.1103/physrevstab.16.111002
- [4] D. Pellegrini, F. Antoniou, S. D. Fartoukh, G. Iadarola, and Y. Papaphilippou, “Multiparametric Response of the LHC Dynamic Aperture in Presence of Beam-Beam Effects”, in *Proc. 8th Int. Particle Accelerator Conf. (IPAC'17)*, Copenhagen, Denmark, May 2017, pp. 2051-2054.  
doi:10.18429/JACoW-IPAC2017-TUPVA009
- [5] N. Karastathis, R. De Maria, S. Fartoukh, Y. Papaphilippou, and D. Pellegrini, “Refining the HL-LHC operational settings with inputs from dynamic aperture simulations: A progress report”, *Journal of Physics: Conference Series*, vol. 1067, p. 022005, Sep. 2018.  
doi:10.1088/1742-6596/1067/2/022005
- [6] G. Arduini *et al.*, “HL-LHC Proton Operation Scenario – Update”, unpublished.
- [7] R. De Maria *et al.*, “SixTrack Version 5: Status and New Developments”, in *Proc. 10th Int. Particle Accelerator Conf. (IPAC'19)*, Melbourne, Australia, May 2019, pp. 3200-3203.  
doi:10.18429/JACoW-IPAC2019-WEPTS043
- [8] J. Laskar, C. Froeschlé, and A. Celletti, “The measure of chaos by the numerical analysis of the fundamental frequencies. application to the standard mapping”, *Physica D: Nonlinear Phenomena*, vol. 56, pp. 253–269, May 1992.  
doi:10.1016/0167-2789(92)90028-L
- [9] Y. Papaphilippou, “Detecting chaos in particle accelerators through the frequency map analysis method”, *Chaos: An Interdisciplinary Journal of Nonlinear Science*, vol. 24, no. 2, p. 024412, 2014. doi:10.1063/1.4884495
- [10] J. Laskar, “Introduction to frequency map analysis”, in *Hamiltonian systems with three or more degrees of freedom*, C. Simó Ed., Dordrecht, Netherlands: Springer, 1999, pp. 134–150.
- [11] J. Laskar, “Frequency Map Analysis and Particle Accelerators”, in *Proc. 20th Particle Accelerator Conf. (PAC'03)*, Portland, OR, USA, May 2003, paper WOAB001, pp. 378–382.
- [12] J. Laskar, “Application of frequency map analysis”, in *The Chaotic Universe: Proc. of the Second ICRA Network Workshop*, Rome, Pescara, Italy, Feb. 1999, vol. 10, p. 115.
- [13] D. Pellegrini *et al.*, “Incoherent beam-beam effects and lifetime optimization”, in *Proc. 9th Evian Workshop on LHC beam operation*, Evian Les Bains, France, Dec. 2017, pp. 93-98.
- [14] S. Kostoglou, “Review of the situation without MS10 at the beginning of collisions and at the end leveling”, presented at 189th HiLumi WP2 Meeting, Geneva, Switzerland, Apr. 2021, unpublished.
- [15] F. Plassard, R. De Maria, and M. Giovannozzi, “Sextupole scheme optimization for HL-LHC”, unpublished.